論文 / 著書情報
Article / Book Information

Title	Composite structure and size effect of barium titanate nanoparticles
Authors	Takuya Hoshina,Satoshi Wada,Yoshihiro Kuroiwa,Takaaki Tsurumi
Citation	Appl. Phys. Lett., Vol. 93, ,
Pub. date	2008, 11
URL	http://scitation.aip.org/content/aip/journal/apl
Copyright	Copyright (c) 2008 American Institute of Physics

Composite structure and size effect of barium titanate nanoparticles

Takuya Hoshina,[1,a)] Satoshi Wada,[2] Yoshihiro Kuroiwa,[3] and Takaaki Tsurumi[1]
[1]*Graduate School of Science and Engineering, Tokyo Institute of Technology, Ookayama, Megoro, Tokyo 152-8552, Japan*
[2]*Interdisciplinary Graduate School of Medical and Engineering, University of Yamanashi, Takeda, Kofu, Yamanashi 400-8511, Japan*
[3]*Graduate School of Science, Hiroshima University, Kagamiyama, Higashi-Hiroshima, Hiroshima 739-8526, Japan*

(Received 30 June 2008; accepted 24 October 2008; published online 13 November 2008)

Nanostructures of barium titanate ($BaTiO_3$) nanoparticles were analyzed using a composite structure model. It was found that $BaTiO_3$ nanoparticles had a composite structure consisting of (i) inner tetragonal core, (ii) gradient lattice strain layer (GLSL), and (iii) surface cubic layer. The crystal structure of each region did not depend on particle size while the volume fraction of the GLSL and the surface cubic layer increased with decreasing the particle size. These results suggested that the size effect of $BaTiO_3$ nanoparticles originated from the composite structure. © *2008 American Institute of Physics*. [DOI: 10.1063/1.3027067]

Ferroelectric $BaTiO_3$ fine particles have been used as raw materials of dielectric devices such as multilayered ceramic capacitors (MLCCs). For the development of future MLCCs as well as other nanodevices, $BaTiO_3$ nanoparticles should be handled and utilized. However, the biggest obstacle in the utilization of dielectric property of nanosized $BaTiO_3$ is the "size effect." Many reports indicated that the dielectric permittivity of $BaTiO_3$ ceramics and powders somehow decreased with decreasing the grain size and the particle size.[1–5] On the contrary, we have demonstrated that the permittivity of $BaTiO_3$ particles showed a maximum value (~5000) at a particle size around 140 nm, which will open a possibility in the applications of $BaTiO_3$ nanoparticles.[6–8] However, the mechanism to explain this anomalous phenomenon and the size effect of $BaTiO_3$ nanoparticles have not been understood so far. In this study, a composite structure model including a gradient lattice strain layer (GLSL) between an inner tetragonal core and a surface cubic layer of $BaTiO_3$ particles was proposed to explain the size effect in $BaTiO_3$ nanoparticles.

It is known that the crystal structure and the dielectric property of $BaTiO_3$ particles depend on impurities and defects in the crystals. Therefore, almost impurity- and defect-free $BaTiO_3$ particles with various sizes should be prepared to investigate the intrinsic size effect of $BaTiO_3$ particles. The two-step decomposition method of barium titanyl oxalate enabled us to synthesize almost impurity- and defect-free $BaTiO_3$ particles with various particle sizes from 20 to 1000 nm.[6,7]

High intensity synchrotron radiation x-ray diffraction (XRD) data of the $BaTiO_3$ particles synthesized by the two-step decomposition method were collected using a Debye–Sherrer camera installed at BL02B2 in the synchrotron radiation facility, SPring-8. High energy x-ray with the wavelength of 0.50 Å was used as the incident beam. Open circles in Figs. 1(a)–1(c) are measured XRD profiles of the $BaTiO_3$ particles with the particle sizes of 85, 140, and 430 nm. The XRD intensity between 002 and 200 diffraction lines increased with decreasing the particle size. At first, we tried to analyze the XRD profiles with the Rietveld method but such intensity bridges between the two diffraction lines could never be fitted by assuming single tetragonal phase or even a surface cubic layer on $BaTiO_3$ particles as shown in previous reports.[9–11] Therefore, we have employed a particle

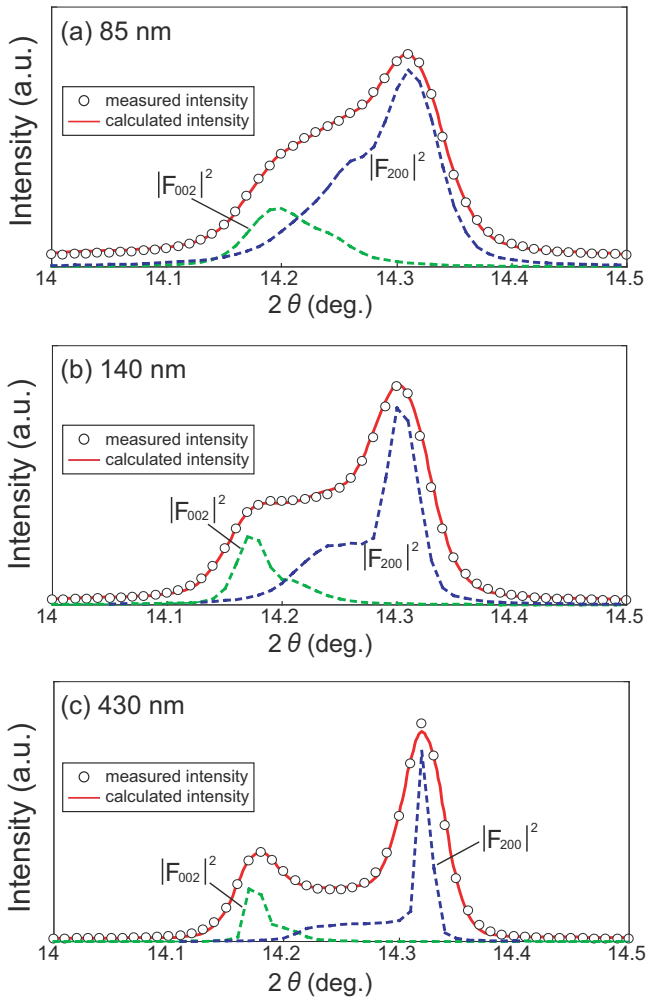

FIG. 1. (Color online) XRD profile around 002 and 200 diffraction lines for $BaTiO_3$ nanoparticles of (a) 85, (b) 140, and (c) 430 nm.

[a)]Electronic mail: hoshina@cim.ceram.titech.ac.jp.

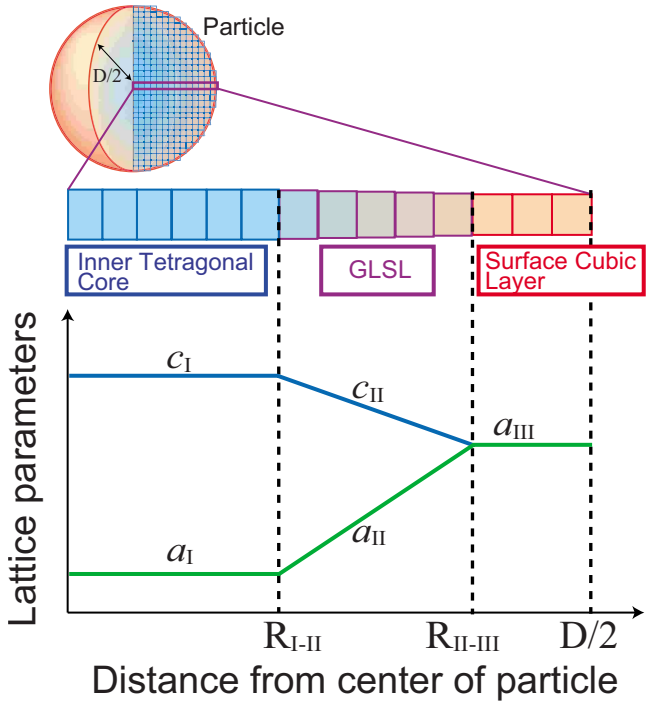

FIG. 2. (Color online) Composite structure model of $BaTiO_3$ nanoparticle.

structure model as shown in Fig. 2, where $BaTiO_3$ particle consisted of three regions, i.e., (i) inner tetragonal core, (ii) GLSL, and (iii) surface cubic layer. This model was designed to incorporate the lattice relaxation[12–14] between the inner tetragonal core and the surface cubic layer. Lattice parameters (*a*-axis and *c*-axis length) and atomic positions were changed continuously in the GLSL. The XRD profiles around 002 and 200 diffraction lines were fitted with those calculated by summing up the crystal structure factors of unit cells over an entire particle as described bellow. First, all lattices of a particle in the *x*-*z* plane were constructed as shown in Fig. 3. The sum total of the crystal structure factors for the lattices which line up at *m*th position shown in Fig. 3 is given by

$$F_m(00l) = \sum_{j,n} f_j \exp\left(2\pi i \frac{\sum_n c_{mn} + z_{mn,j} c_{mn}}{d}\right), \tag{1}$$

where f_j is the atomic scattering factor of the *j*th atom, c_{mn} and z_{mnj} are, respectively, the *c*-axis length and the atomic

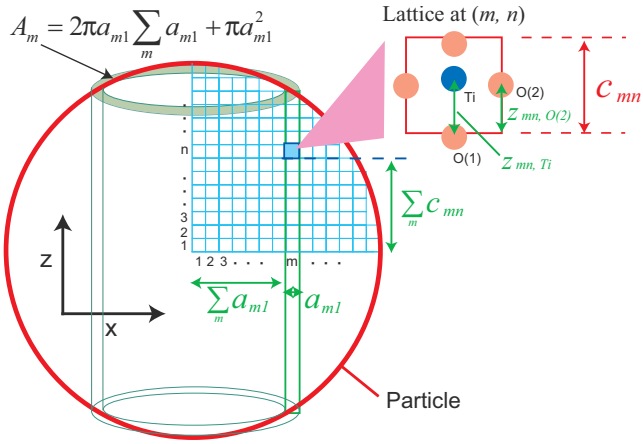

FIG. 3. (Color online) Calculation of crystal structure factor for $BaTiO_3$ particle with composite structure.

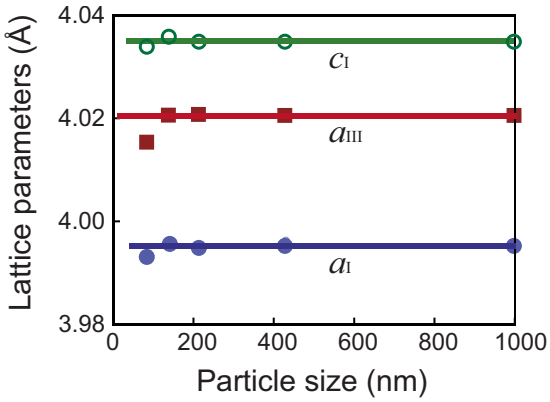

FIG. 4. (Color online) Particle size dependence of lattice parameters of inner tetragonal core (a_I and c_I) and surface cubic layer (a_{III}).

position along the *z*-axis of the lattice at (m,n) position, and *d* is the *d*-spacing expressed by Bragg's law. The total intensity of 00*l* diffraction from the entire particle was approximately calculated by summing up the intensity from the cylinder segments shown in Fig. 3.

$$I'(00l) \approx \sum_m A_m |F_m(00l)|^2, \tag{2}$$

$$A_m = 2\pi a_{m1} \sum_m a_{m1} + \pi a_{m1}^2, \tag{3}$$

where a_{m1} is the *a*-axis length of the lattice at $(m,1)$ position. In a similar way, the total intensity, $I'(h00)$ of *h*00 diffraction from the entire particle was also calculated. In tetragonal phase, the total intensity around 00*l* and *h*00 diffractions was theoretically calculated as follows:

$$I'_{\text{calc}} = 2I'(h00) + I'(00l). \tag{4}$$

The observed XRD profiles were fitted to the following calculated intensity under consideration of the diffraction lines broadening due to the measurement system and background

$$I_{\text{calc}} \approx s\Phi I'_{\text{calc}} + y_b, \tag{5}$$

where *s* is the scale parameter, Φ is the Gaussian function, and y_b is the background parameter. In the nonlinear least fitting process, several parameters such as *a*-axis length of inner tetragonal core (a_I), *c*-axis length of inner tetragonal core (c_I), *a*-axis length of surface cubic layer (a_{III}), the distance from the center to the boundary between inner tetragonal core and GLSL ($R_{I\text{-}II}$), and the distance from the center to the boundary between GLSL and surface cubic layer ($R_{II\text{-}III}$) were optimized. The programming code for the calculation and the fitting of XRD profiles was developed in this study. Solid lines in Fig. 1 show the fitting results for the $BaTiO_3$ particles with different particle sizes. Very good fittings could be obtained using the composite structure model with the GLSL, which gave the evidence that $BaTiO_3$ nanoparticles had composite structures composed of (i) inner tetragonal core, (ii) GLSL, and (iii) surface cubic layer.

Figure 4 shows the lattice parameters of the inner tetragonal core (a_I and c_I) and the surface cubic layer (a_{III}). It should be noted that the lattice parameters of the inner tetragonal core and the surface cubic layer were independent of the particle size. Previous studies reported that the c/a ratio of $BaTiO_3$ particles decreased with particle size[7,8,12,15]

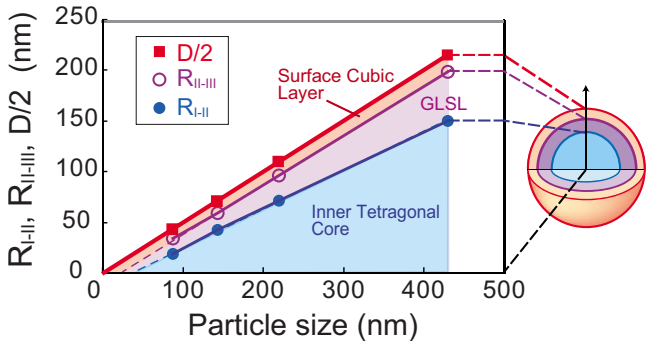

FIG. 5. (Color online) Particle size dependence of the thickness of inner tetragonal core, GLSL, and surface cubic layer.

and usually the c/a ratio was used as an index to filter the high grade $BaTiO_3$ particles in MLCC industry.[5] However, this study revealed that the lattice parameters of the inner tetragonal core were almost consistent with that of $BaTiO_3$ bulk single crystal.[16] The particle size dependence of the c/a ratio should be interpreted as the change in the volume fraction of the surface cubic layer. On the other hand, the lattice parameter of the surface cubic layer was close to that of $BaTiO_3$ nanoparticles with a particle size around 20 nm (Ref. 8) and the unit cell volume of the surface cubic layer was larger than that of bulk crystal, indicating that a lattice expansion occurred on the surface of the $BaTiO_3$ nanoparticles.

Figure 5 shows the size dependence of the thicknesses of the three regions $R_{I\text{-}II}$ ($R_{II\text{-}III}$-$R_{I,II}$) and ($D/2-R_{I\text{-}II}$), where $R_{I\text{-}II}$ is the radius of the inner tetragonal core, ($R_{II\text{-}III}$-$R_{I,II}$) is the thickness of the GLSL and ($D/2$-$R_{I\text{-}II}$) is the thickness of the surface cubic layer. It was found that the thickness of the surface cubic layer was almost constant (10–15 nm) despite particle size. This means that the ferroelectricity of the $BaTiO_3$ powders should disappear below the particle size of 20–30 nm because the particles loses tetragonal core below this size. The existence of ferroelectric critical size was pointed out in previous studies.[15,17] The ferroelectric critical size, 20–30 nm, determined in this study was consistent with that estimated by the symmetry assignment in XRD analysis for the same samples.[8] In the size effect of $BaTiO_3$ particles, the crystal structures of the three regions did not depend on particle sizes while only the volume fraction of the these regions changes with particle size. The ferroelectricity is depressed with decreasing the particle size and finally disappears below the critical size. This phenomenon was explained by the increase in the volume fraction of the surface cubic layer with decreasing the particle size.

The composite structure suggests that the dielectric property of $BaTiO_3$ particles is dependent on the particle size. The dielectric permittivity of the surface cubic layer must be lower than that of the bulk crystal because the surface cubic layer is a paraelectric layer. On the other hand, we believe GLSL has high permittivity because the GLSL is the static phase transitional layer from the tetragonal phase to the cubic phase. We observed a decreasing of the soft-mode frequency, which was the origin of the enhancement in dielectric permittivity, with decreasing the particle size in previous study.[18,19] We think that the decreasing of the soft-mode frequency is due to the increase in the volume fraction of GLSL. The GLSL enhanced the permittivity while the surface cubic layer depressed it. By assuming the abovementioned dielectric distribution inside a particle, the particle size dependence of the permittivity may be explained from the size dependence of the volume fractions of GLSL and surface cubic layer.

We conclude that $BaTiO_3$ nanoparticles had the composite structure consisting of (i) inner tetragonal core, (ii) GLSL, and (iii) surface cubic layer. The crystal structures of the three regions did not depend on particle sizes while only the volume fractions of these regions changed with particle size. These results suggested that the size effect of $BaTiO_3$ nanoparticles originated from the composite structure.

This work was supported by the Grant-in-Aid for Scientific Research of the Japan Society for the Promotion of Science. The synchrotron radiation experiment was performed at the BL02B2 in the SPring-8 with the approval of the Japan Synchrotron Radiation Research Institute (Program No. 2006A1618).

[1] G. Arlt, D. Hennings, and G. De With, J. Appl. Phys. **58**, 1619 (1985).
[2] M. H. Frey and D. A. Payne, Phys. Rev. B **54**, 3158 (1996).
[3] A. V. Polotai, A. V. Ragulya, and C. A. Randall, Ferroelectrics **288**, 93 (2003).
[4] Z. Zhao, V. Buscaglia, M. Viviani, M. T. Buscaglia, L. Mitoseriu, A. Testino, M. Nygren, M. Johnsson, and P. Nanni, Phys. Rev. B **70**, 024107 (2004).
[5] T. Tsurumi, T. Sekine, H. Kakemoto, T. Hoshina, S.-M. Nam, H. Yasuno, and S. Wada, J. Am. Ceram. Soc. **89**, 1337 (2006).
[6] T. Hoshina, H. Yasuno, S.-M. Nam, H. Kakemoto, T. Tsurumi, and S. Wada, Trans. Mater. Res. Soc. Jpn. **29**, 1207 (2004).
[7] S. Wada, T. Hoshina, H. Yasuno, S.-M. Nam, H. Kakemoto, T. Tsurumi, and M. Yashima, J. Korean Phys. Soc. **46**, 303 (2005).
[8] T. Hoshina, H. Kakemoto, T. Tsurumi, S. Wada, and M. Yashima, J. Appl. Phys. **99**, 054311 (2006).
[9] S. Aoyagi, Y. Kuroiwa, A. Sawada, I. Yamashita, and T. Atake, J. Phys. Soc. Jpn. **71**, 1218 (2002).
[10] Y. Kuroiwa, S. Aoyagi, A. Sawada, H. Ikawa, I. Yamashita, N. Inoue, and T. Atake, J. Therm. Anal. Calorim. **69**, 933 (2002).
[11] T. Hoshina, H. Kakemoto, T. Tsurumi, S. Wada, M. Yashima, K. Kato, and M. Takata, Key Eng. Mater. **301**, 239 (2006).
[12] K. Ishikawa and T. Uemori, Phys. Rev. B **60**, 11841 (1999).
[13] W. L. Zhong, Y. G. Wang, P. L. Zhang, and B. D. Qu, Phys. Rev. B **50**, 698 (1994).
[14] B. Jiang and L. A. Bursill, Phys. Rev. B **60**, 9978 (1999).
[15] K. Uchino, E. Sadanaga, and T. Hirose, J. Am. Ceram. Soc. **72**, 1555 (1989).
[16] H. F. Kay and P. Vousden, Philos. Mag. **40**, 1019 (1949).
[17] K. Ishikawa, K. Yoshikawa, and N. Okada, Phys. Rev. B **37**, 5852 (1988).
[18] T. Hoshina, H. Yasuno, H. Kakemoto, T. Tsurumi, and S. Wada, Ferroelectrics **353**, 55 (2007).
[19] T. Hoshina, H. Kakemoto, T. Tsurumi, and S. Wada, Key Eng. Mater. **350**, 47 (2007).